Signal Processing 180 (2021) 107891

Contents lists available at ScienceDirect

Signal Processing

journal homepage: www.elsevier.com/locate/sigpro

Power-based Capon beamforming: Avoiding the cancellation effects of GNSS multipath

Martí Mañosas-Caballú [a,*], A. Lee Swindlehurst [b], Gonzalo Seco-Granados [a]

[a] Dpt. Telecomm. and Syst. Engineering, Universitat Autònoma de Barcelona, Spain
[b] Dpt. Electrical Engineering and Comp. Science, University of California at Irvine, United States

A R T I C L E I N F O

Article history:
Received 25 March 2020
Revised 7 August 2020
Accepted 5 November 2020
Available online 10 November 2020

Keywords:
Beamforming
Capon
Arrays
Multipath
Correlated
Coherent
GNSS
Time-delay
Carrier-phase

A B S T R A C T

This paper addresses the problem of GNSS multipath mitigation using antenna arrays. A new data-dependent beamforming technique is proposed that is based on the well-known Capon beamformer. This technique aims to avoid the typical cancellation phenomenon between signal and correlated multipaths, by exploiting the known power of the direct signal at the receiver. To this effect, a measure of the correlation between the signal and multipaths is obtained in matrix form, and it is then subtracted from the spatial correlation matrix of the received signal. This results in a new spatial correlation matrix that is used for the final Power-Based Capon beamformer. The behaviour of this technique is justified mathematically, and it is supported by several numerical results. These results show that the obtained multipath attenuations are generally superior to those obtained by other existing techniques, and also that the noise response is very satisfactory. The impact of the proposed technique on the time-delay and carrier-phase calculation at the GNSS receiver is also considered. While the obtained carrier-phase observables are reasonably accurate, the final distortion on the time-delay is exceptionally low for any multipath delay.

1. Introduction

Global Navigation Satellite Systems (GNSS) enable the calculation of a user position by using the signals transmitted by a constellation of specific satellites. In order to obtain this position, some essential parameters have to be estimated at the user receiver. For instance, the time-delay of the received signals is very important, and it has a great impact on the receiver accuracy. It is used for the calculation of the *pseudorange*, or apparent distance between the user and each available satellite. This distance does not typically match with the exact geometric distance due to, among other factors, synchronism errors between the receiver and satellite clocks, but it leads to a system of equations from which the position can be calculated [1]. The carrier-phase of the received signals may also be used to obtain a measure of the distance between the satellite and receiver, and it is particularly appealing because it provides a much more precise measurement than the time-delay. However, it also presents some limitations, such as being ambiguous by an unknown integer number of wavelengths.

For GNSS, only the received Line-Of-Sight Signal (LOSS) is exploited to obtain useful information about the receiver position. Multipath reflections usually bias the time-delay and carrier-phase estimates, so that pseudoranges may change by several tens of meters, and they also hamper the ambiguity resolution process needed for carrier-phase ranging [2]. For this reason, significant research and development efforts have been devoted to the mitigation of multipath effects, and many techniques have been proposed so far. On one hand, there are single-antenna techniques, which attempt to discriminate the LOSS from the reflections by exploiting their temporal diversity. Examples of such techniques are the narrow-correlator [3], the strobe-correlator [4] and the MEDLL [5], but there are other proposals as well [6–8]. Although these approaches improve on the standard positioning accuracy, their performance is still insufficient for many precise applications. On the other hand, there are multiple-antenna techniques, which exploit the spatial diversity, and are able to discriminate the reflections when they come from different directions [9]. So far, several multiple-antenna studies have been proposed that take into account the underlying particularities of a GNSS scenario. These include the application of the basic Howells-Applebaum and Power-Inversion methods [10], the use of Deterministic Beamforming techniques [11], specific methods based on Maximum Likelihood (ML) estimation [12], two-step approaches based on Eigen-decomposition [13], and many other examples [14–16]. A thor-

* Corresponding author.
E-mail addresses: marti.manosas@e-campus.uab.cat (M. Mañosas-Caballú), swindle@uci.edu (A.L. Swindlehurst), gonzalo.seco@uab.cat (G. Seco-Granados).

https://doi.org/10.1016/j.sigpro.2020.107891
0165-1684/

ough overview can be found in [17], and other recent studies are [18] and [19].

Overall, the best and most well-known multiple-antenna solutions are based on data-dependent beamforming, where the optimal beamforming weights depend on the statistics of the incoming data [9]. They are very appropriate for situations where little a priori information about the scenario is available, or when the scenario is likely to change with time. When the spatial and/or temporal signatures of the LOSS are assumed known, it is common to exploit them to improve performance at the output of the array [20]. Otherwise, there are also blind beamforming techniques that only exploit some specific properties of the involved signals, such as constant modulus and self-coherence, and hence they are robust to errors in the previous assumptions. In any case, the data that is used to compute the beamforming weights can be obtained either before or after the despreading process, since all present and planned navigation systems use Direct-Sequence Spread-Spectrum (DS-SS) signals. When mitigating the multipath is the main issue, it is recommended to employ the post-despreading signals because the despreading makes the multipath contribution more noticeable. The weights can then be applied to either the pre-despreading or the post-despreading signals.

Although data-dependent beamforming is very useful in many situations, it often fails when very correlated signals are present. Hence, it is not useful to mitigate multipath reflections with very small delay relative to the LOSS. For this reason, some robust beamforming techniques that combat highly correlated signals have been proposed, but they still present certain limitations. The first remarkable contribution was in 1982, with the work of Widrow et al. [21]. Then, Shan et al. [22] introduced the powerful spatial smoothing technique for Direction-Of-Arrival (DOA) estimation, which satisfactorily decorrelates a set of coherent signals impinging on an antenna array. However, the application of this technique to the beamforming problem involves a regular array geometry, such as a uniform linear array or a uniform rectangular array, and it also requires using a large amount of sensors. Other interesting alternatives were presented by Bresler et al. [23] afterwards. Also, a forward/backward extension of the spatial smoothing technique was presented in [24], which reduces the number of extra sensors needed for decorrelation. A ML estimation procedure for the location of coherent sources was presented in [25], and a quadratically constrained approach was implemented in [26]. Other important works have also been presented since [27–30]. Nonetheless, there is still no method that satisfactorily mitigates the effects of the multipath on the pseudoranges for all possible relative delays, unless it is at the expense of a loss of the array resolution or the computational need to estimate the DOA of each multipath.

Noteworthy characteristic of GNSS is that receivers are continuously provided with accurate information of the satellites' positions and with their own position estimates. Often, this particularity is exploited to calculate some useful parameters at the receiver for data-dependent beamforming. For instance, the DOA of the direct signal. Note that in very adverse multipath scenarios, the inaccuracies of the receiver and satellite positions are at most on the order of a few hundred meters, and hence they are not important in determining the DOA. In fact, many beamforming techniques use this parameter together with the known geometry of the array to determine the spatial signature of the LOSS [20]. The assumption of a known spatial signature relies on the availability of array calibration, since some modelling errors always exist that must be taken into account. This problem can be found in many applications of antenna arrays, and robust calibration methods developed for generic applications are also applicable here.. Finally, note that in very adverse multipath scenarios, the inaccuracies of the receiver and satellite positions are at most on the order of a few hundred meters, and hence they are not important in determining the DOA of the signal.

In a similar manner to the DOA, the theoretical value of the received power of the LOSS can also be calculated at the receiver. In this case, the knowledge of the satellite transmit power and a proper model for the direct-path loss are fundamental, in addition to the distance between the receiver and the satellite that is obtained from the receiver and satellite positions. The errors in the receiver position, even if they are on the order of hundreds of meters, have no significant impact on the calculation of the distance because the satellites are 20000 km or further way. Only the deviations due to model mismatches need to be considered, which can be further reduced by contrasting them with previous estimation records and some specific template functions [31]. Note that the knowledge of the LOSS power occurs on top of the more usual assumption that the noise power at each element of the array can be estimated, and we aim to show that it has a great potential to reduce the multipath effects. .

In this paper, we propose a new data-dependent beamformer that exploits the previous GNSS particularities. The proposed technique is based on the well-known Capon beamformer [32], and it uses the post-despreading signals to calculate the weights. In particular, it attempts to attenuate interference, multipath and noise, exploiting the fact that the spatial signature and power of the LOSS are known at the receiver. In the next section, the model of the problem is presented formally. Then, a novel review of the Capon beamformer in the presence of multipaths follows. This new look motivates the proposed Power-Based Capon (PBC) beamformer, which is detailed in Section 4. Afterwards, some simulation results are presented, which demonstrate the behaviour of our methodology. Finally, conclusions about the work are drawn in Section 6.

2. Problem model

Let us consider that an arbitrary N-element antenna array receives the DS-SS signal transmitted by a given GNSS satellite together with $D < N$ multipath reflections. After the despreading process, the nth sample of the data received by the array is modeled as:

$$\mathbf{x}[n] = \mathbf{a}s[n] + \mathbf{B}\mathbf{m}[n] + \mathbf{v}[n] \tag{1}$$

where $s[n] \in \mathbb{C}$ is the LOSS, $\mathbf{a} \in \mathbb{C}^N$ is its corresponding spatial signature, $\mathbf{m}[n] := [m_1[n] \dots m_D[n]]^T$ is a vector containing all multipath contributions $m_k[n] \in \mathbb{C}$ for $k = 1, \dots, D$, the matrix $\mathbf{B} := [\mathbf{b}_1 \dots \mathbf{b}_D]$ contains at each column the spatial signature of each multipath, and $\mathbf{v}[n] \in \mathbb{C}^N$ is the received noise at each element of the array, which is assumed to be spatially white and with identical noise power at each sensor. In the scenario of interest, the multipath reflections can be either correlated or uncorrelated with the direct signal. When one or more reflections have zero relative delay, we refer to it as the coherent multipath case. As all the involved signals are assumed to impinge on the array from different directions, in this work we assume that $\mathbf{a}$, $\mathbf{b}_1, \dots, \mathbf{b}_D$ are linearly independent vectors. In addition, $\mathbf{a}$ is considered known, whereas $\mathbf{b}_1, \dots, \mathbf{b}_D$ are unknown.

We process $\mathbf{x}[n]$ through a given *beamforming* technique, which uses some complex weights $\mathbf{w} \in \mathbb{C}^N$ to generate the signal $y[n] = \mathbf{w}^H\mathbf{x}[n]$ at the output of the processor. The purpose of this operation is to mitigate the multipath contribution, interference and noise, while keeping $s[n]$ undistorted. Then, the time-delay and carrier-phase of the LOSS can be estimated from $y[n]$, which are usually fed back to the despreading stage as illustrated in Fig. 1. A very interesting approach for the beamforming stage is the Capon beamformer, which calculates w from the solution to:

$$\min_{\mathbf{w}} \ \mathbf{w}^H\mathbf{R}_{\mathbf{xx}}\mathbf{w} \text{ subject to } \mathbf{w}^H\mathbf{a} = 1 \tag{2}$$

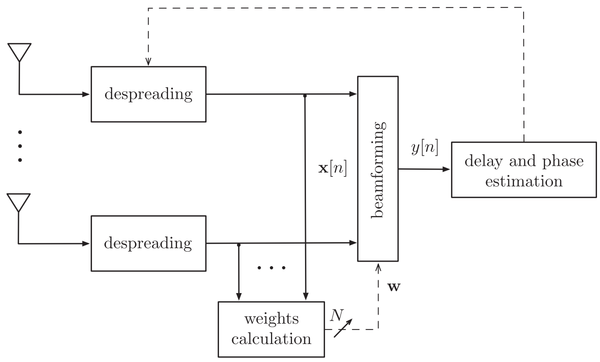

Fig. 1. Proposed GNSS multiple-antenna receiver.

where $\mathbf{R_{xx}} = \mathrm{E}\{\mathbf{x}[n]\mathbf{x}[n]^H\}$ is the spatial correlation matrix of $\mathbf{x}[n]$. This problem minimizes the output power $\sigma_y^2 = \mathrm{E}\{|y[n]|^2\}$ using the distortionless constraint $\mathbf{w}^H\mathbf{a} = 1$, aiming to place nulls at the directions of the interference and to keep the signal $s[n]$ undistorted. Unfortunately, it is well-known that (2) does not work properly in the presence of correlated multipaths, since it cancels them together with $s[n]$, and hence it eliminates the contribution of $s[n]$, at the output.

In this work, we seek a solution to this cancellation phenomenon of the Capon beamformer. Concretely, we aim to identify in $\mathbf{R_{xx}}$ the portion of the multipaths that contributes to the cancellation, and then counteract it before calculating the Capon weights. As a key aspect of the proposed procedure is to exploit the fact that the power of the LOSS is known at the receiver, we refer to the approach as Power-Based Capon beamforming.

3. Capon beamforming review

We begin with the general expression of the spatial correlation matrix of $\mathbf{x}[n]$:

$$\mathbf{R_{xx}} = \sigma_s^2\mathbf{a}\mathbf{a}^H + \mathbf{a}\mathbf{r}_{\mathbf{m}s}^H\mathbf{B}^H + \mathbf{B}\mathbf{r}_{\mathbf{m}s}\mathbf{a}^H + \mathbf{B}\mathbf{R_m}\mathbf{B}^H + \sigma_v^2\mathbf{I} \tag{3}$$

where σ_s^2 is the power of the signal $s[n]$, σ_v^2 is the power of the noise $\mathbf{v}[n]$, $\mathbf{r}_{\mathbf{m}s} = \mathrm{E}\{\mathbf{m}[n]s[n]^*\}$ contains the correlation between the LOSS and its multipaths, $\mathbf{R_m} = \mathrm{E}\{\mathbf{m}[n]\mathbf{m}[n]^H\}$ is the correlation matrix of the multipaths, and $\mathbf{I}$ is the identity matrix. From this expression, we can illustrate two different scenarios that explain the cancellation phenomenon of the Capon beamformer. They are based on the value of $\mathbf{r}_{\mathbf{m}s}$, taking into account that the power at the output of the beamformer $\sigma_y^2 = \mathbf{w}^H\mathbf{R_{xx}}\mathbf{w}$ is minimized and the distortionless constraint $\mathbf{w}^H\mathbf{a} = 1$ is verified.

When the direct signal is uncorrelated with its multipaths, $\mathbf{r}_{\mathbf{m}s} = \mathbf{0}$, and the spatial correlation matrix becomes $\mathbf{R_{xx}} = \sigma_s^2\mathbf{a}\mathbf{a}^H + \mathbf{B}\mathbf{R_m}\mathbf{B}^H + \sigma_v^2\mathbf{I}$. As a result, the power at the output of the beamformer can be written as:

$$\sigma_y^2 = \sigma_s^2 + \mathbf{w}^H\mathbf{B}\mathbf{R_m}\mathbf{B}^H\mathbf{w} + \sigma_v^2\|\mathbf{w}\|^2 \tag{4}$$

Eq. (4) shows that the power at the output of the beamformer is the contribution of the power of the LOSS, the multipaths and the noise separately. Note that $\sigma_s^2 > 0$, $\mathbf{w}^H\mathbf{B}\mathbf{R_m}\mathbf{B}^H\mathbf{w} \geq 0$ and $\sigma_v^2\|\mathbf{w}\|^2 > 0$, so the weights $\mathbf{w}$ cannot mix the direct signal with the multipaths and noise at the output to reduce the power σ_y^2, but instead they can only reduce the multipaths and noise individually.

In contrast, when the direct signal and its multipaths are correlated, $\mathbf{r}_{\mathbf{m}s} \neq \mathbf{0}$. Then, the power at the output is given by:

$$\sigma_y^2 = \sigma_s^2 + \mathbf{w}^H\mathbf{a}\mathbf{r}_{\mathbf{m}s}^H\mathbf{B}^H\mathbf{w} + \mathbf{w}^H\mathbf{B}\mathbf{r}_{\mathbf{m}s}\mathbf{a}^H\mathbf{w} + \mathbf{w}^H\mathbf{B}\mathbf{R_m}\mathbf{B}^H\mathbf{w} + \sigma_v^2\|\mathbf{w}\|^2 \tag{5}$$

Eq. (5) shows that the power at the output it is not just formed by the contribution of the LOSS, multipaths and noise separately, but it also contains the term $\mathbf{w}^H\mathbf{a}\mathbf{r}_{\mathbf{m}s}^H\mathbf{B}^H\mathbf{w} + \mathbf{w}^H\mathbf{B}\mathbf{r}_{\mathbf{m}s}\mathbf{a}^H\mathbf{w}$, which is due to the correlation between the direct signal and multipaths. This term is real and can be negative, so the weights $\mathbf{w}$ can mix it with the contribution of the direct signal and multipaths at the output in order to reduce the power σ_y^2. This is the well-known cancellation phenomenon of the Capon beamformer, and as we have seen it is due to the existence of a non-zero $\mathbf{r}_{\mathbf{m}s}$.

4. Power-based Capon beamforming

As we have seen in the previous section, the value of $\mathbf{r}_{\mathbf{m}s}$ in (3) determines the behaviour of the Capon beamformer in the presence of multipaths, and the cancellation phenomenon only appears when $\mathbf{r}_{\mathbf{m}s} \neq 0$. Therefore, a reasonable approach to avoid the cancellation is to eliminate the contribution of $\mathbf{r}_{\mathbf{m}s}$ from the correlation matrix $\mathbf{R_{xx}}$. In order to eliminate this contribution, the Power-Based Capon beamformer calculates the terms $\mathbf{a}\mathbf{r}_{\mathbf{m}s}^H\mathbf{B}^H$ and $\mathbf{B}\mathbf{r}_{\mathbf{m}s}\mathbf{a}^H$, and subtracts them from $\mathbf{R_{xx}}$. Since $\mathbf{a}$ is known and $\mathbf{B}$ is unknown, we estimate the cross-correlation parameter $\boldsymbol{\alpha}_0 := \mathbf{B}\mathbf{r}_{\mathbf{m}s}$, and then calculate the terms $\mathbf{a}\boldsymbol{\alpha}_0^H$ and $\boldsymbol{\alpha}_0\mathbf{a}^H$.

4.1. Cross-correlation estimation

In order to estimate $\boldsymbol{\alpha}_0$, we first generate a modified correlation matrix $\mathbf{C_{xx}}$ defined as:

$$\mathbf{C_{xx}} := \mathbf{R_{xx}} - \sigma_s^2\mathbf{a}\mathbf{a}^H - \sigma_v^2\mathbf{I} \tag{6}$$

where both the power of the direct signal σ_s^2 and the power of the noise σ_v^2 need to be used. This allows us to work with a matrix with the following structure:

$$\mathbf{C_{xx}} = \begin{bmatrix}\mathbf{a} & \mathbf{B}\end{bmatrix}\begin{bmatrix}0 & \mathbf{r}_{\mathbf{m}s}^H \\ \mathbf{r}_{\mathbf{m}s} & \mathbf{R_m}\end{bmatrix}\begin{bmatrix}\mathbf{a}^H \\ \mathbf{B}^H\end{bmatrix}$$

where the term $\mathbf{r}_{\mathbf{m}s}$ appears somewhat isolated. Then, if we subtract the term $\mathbf{a}\boldsymbol{\alpha}_0^H + \boldsymbol{\alpha}_0\mathbf{a}^H$ from $\mathbf{C_{xx}}$, we obtain:

$$\mathbf{C_{xx}} - \mathbf{a}\boldsymbol{\alpha}_0^H - \boldsymbol{\alpha}_0\mathbf{a}^H = \begin{bmatrix}\mathbf{a} & \mathbf{B}\end{bmatrix}\begin{bmatrix}0 & \mathbf{0}^H \\ \mathbf{0} & \mathbf{R_m}\end{bmatrix}\begin{bmatrix}\mathbf{a}^H \\ \mathbf{B}^H\end{bmatrix}$$

which indicates that the rank of $\mathbf{C_{xx}}$ has been decreased. Based on this observation, it is then natural to think that $\boldsymbol{\alpha} = \boldsymbol{\alpha}_0$ may minimize the rank of $\mathbf{C_{xx}} - \mathbf{a}\boldsymbol{\alpha}^H - \boldsymbol{\alpha}\mathbf{a}^H$. In order to understand when this minimization occurs, the following lemma has been developed. Note that $\mathcal{R}(q)$ indicates the real part of q.

Lemma 1. *The rank of the matrix $\mathbf{C_{xx}} - \mathbf{a}\boldsymbol{\alpha}^H - \boldsymbol{\alpha}\mathbf{a}^H$ attains its minimum if and only if $\boldsymbol{\alpha} = \boldsymbol{\alpha}_0 - q\mathbf{a} - \mathbf{B}\mathbf{R_m}\mathbf{p}$ with $q \in \mathbb{C}$, $\mathbf{p} \in \mathbb{C}^D$ such that $\mathbf{p}^H\mathbf{R_m}\mathbf{p} = 2\mathcal{R}\{q\}$.*

Proof. First assume that $\boldsymbol{\alpha}_0 - \boldsymbol{\alpha} \in \mathrm{span}\{\mathbf{a}, \mathbf{B}\}$. Then $\exists\, q \in \mathbb{C}, \mathbf{z} \in \mathbb{C}^D$ such that $\boldsymbol{\alpha}_0 - \boldsymbol{\alpha} = q\mathbf{a} + \mathbf{B}\mathbf{z}$. Then $\mathbf{C_{xx}} - \mathbf{a}\boldsymbol{\alpha}^H - \boldsymbol{\alpha}\mathbf{a}^H$ can be written as:

$$\mathbf{C_{xx}} - \mathbf{a}\boldsymbol{\alpha}^H - \boldsymbol{\alpha}\mathbf{a}^H = \begin{bmatrix}\mathbf{a} & \mathbf{B}\end{bmatrix}\begin{bmatrix}2\mathcal{R}\{q\} & \mathbf{z}^H \\ \mathbf{z} & \mathbf{R_m}\end{bmatrix}\begin{bmatrix}\mathbf{a}^H \\ \mathbf{B}^H\end{bmatrix}$$

As $\mathbf{a}$ and $\mathbf{b}_1, \ldots, \mathbf{b}_D$ are linearly independent, the rank of $\mathbf{C_{xx}} - \mathbf{a}\boldsymbol{\alpha}^H - \boldsymbol{\alpha}\mathbf{a}^H$ is the same as the rank of $\begin{bmatrix}2\mathcal{R}\{q\} & \mathbf{z}^H \\ \mathbf{z} & \mathbf{R_m}\end{bmatrix}$, see [33], which is equal to rank $(\mathbf{R_m})$ if and only if $\exists\, \mathbf{p} \in \mathbb{C}^D$ such that $\mathbf{z} = \mathbf{R_m}\mathbf{p}$ and $2\mathcal{R}\{q\} = \mathbf{z}^H\mathbf{p}$. In the case that there does not exist such $\mathbf{p}$, the rank is equal to $\mathrm{rank}(\mathbf{R_m}) + 1$.

Now assume that $\boldsymbol{\alpha}_0 - \boldsymbol{\alpha} \notin \mathrm{span}\{\mathbf{a}, \mathbf{B}\}$. In this case we cannot write $\boldsymbol{\alpha}_0 - \boldsymbol{\alpha}$ as a linear combination of $\mathbf{a}, \mathbf{B}$. Instead, we must say that $\boldsymbol{\alpha}_0 - \boldsymbol{\alpha}$ is linearly independent of $\mathbf{a}, \mathbf{B}$. Then $\mathbf{C_{xx}} - \mathbf{a}\boldsymbol{\alpha}^H - \boldsymbol{\alpha}\mathbf{a}^H$

can be written as:

$$\mathbf{C_{xx}} - \mathbf{a}\boldsymbol{\alpha}^H - \boldsymbol{\alpha}\mathbf{a}^H = \begin{bmatrix} \boldsymbol{\alpha}_0 - \boldsymbol{\alpha} & \mathbf{a} & \mathbf{B} \end{bmatrix} \begin{bmatrix} 0 & 1 & 0 & \dots & 0 \\ 1 & 0 & 0 & \dots & 0 \\ 0 & 0 & & & \\ \vdots & \vdots & & \mathbf{R_m} & \\ 0 & 0 & & & \end{bmatrix} \begin{bmatrix} \boldsymbol{\alpha}_0^H - \boldsymbol{\alpha}^H \\ \mathbf{a}^H \\ \mathbf{B}^H \end{bmatrix}$$

As $\boldsymbol{\alpha}_0 - \boldsymbol{\alpha}$, $\mathbf{a}$ and $\mathbf{b}_1, \dots, \mathbf{b}_D$ are linearly independent, the rank of the previous matrix is the same as the rank of $\begin{bmatrix} 0 & 1 & 0 & \dots & 0 \\ 1 & 0 & 0 & \dots & 0 \\ 0 & 0 & & & \\ \vdots & \vdots & & \mathbf{R_m} & \\ 0 & 0 & & & \end{bmatrix}$, which is equal to $\text{rank}(\mathbf{R_m}) + 2$.

As a result, we see that the minimum achievable rank is $\text{rank}(\mathbf{R_m})$, and that this is attained if and only if $\boldsymbol{\alpha}_0 - \boldsymbol{\alpha} = q\mathbf{a} + \mathbf{Bz}$ with $\mathbf{z} = \mathbf{R_m p}$ and $2\mathcal{R}\{q\} = \mathbf{z}^H\mathbf{p}$, or equivalently, when $\boldsymbol{\alpha}_0 - \boldsymbol{\alpha} = q\mathbf{a} + \mathbf{BR_m p}$ with $\mathbf{p}^H\mathbf{R_m p} = 2\mathcal{R}\{q\}$. □

Lemma 1 shows us that, effectively, $\boldsymbol{\alpha} = \boldsymbol{\alpha}_0$ minimizes the rank of $\mathbf{C_{xx}} - \mathbf{a}\boldsymbol{\alpha}^H - \boldsymbol{\alpha}\mathbf{a}^H$. In addition, it also tells us that an infinite set of possible $\boldsymbol{\alpha}$ exist that minimize the rank, and it gives us a characterisation of them. As a result, we can try to find the solution $\boldsymbol{\alpha}_0$ by minimizing the rank of $\mathbf{C_{xx}} - \mathbf{a}\boldsymbol{\alpha}^H - \boldsymbol{\alpha}\mathbf{a}^H$, but some additional information should be used. Along these lines, next we construct a parametrisation for $\boldsymbol{\alpha}$ that is based on the fact that the received signals are DS-SS, and the corresponding waveforms are known by the receiver. In particular, we exploit the fact that a replica of the post-despreading signal $s[n]$ can be created by the receiver, with only some unknown delay τ_e and phase φ_e synchronization errors.

We can assume then that a reference signal $c[n] = 1/\sqrt{\sigma_s^2}s[n+\tau_e]e^{-j\varphi_e}$ is available at the receiver. If we correlate it with the received data $\mathbf{x}[n]$ of (1), then we can obtain the following correlation vector:

$$\mathbf{r_{xc}} := \mathrm{E}\{\mathbf{x}[n]c^*[n]\} = \frac{e^{j\varphi_e}}{\sqrt{\sigma_s^2}} r_s(\tau_e)\mathbf{a} + \frac{e^{j\varphi_e}}{\sqrt{\sigma_s^2}} \mathbf{B}\mathbf{r}_{\mathbf{m}s}(\tau_e)$$

where $r_s(\tau_e) = \mathrm{E}\{s[n]s^*[n+\tau_e]\}$ and $\mathbf{r}_{\mathbf{m}s}(\tau_e) = \mathrm{E}\{\mathbf{m}[n]s^*[n+\tau_e]\}$. Then, by tuning the delay and phase of the reference by an amount τ and φ, we can generate the following correlation vectors:

$$\mathbf{r_{xc}}(\tau,\varphi) = \frac{e^{j(\varphi_e-\varphi)}}{\sqrt{\sigma_s^2}} r_s(\tau_e-\tau)\mathbf{a} + \frac{e^{j(\varphi_e-\varphi)}}{\sqrt{\sigma_s^2}} \mathbf{B}\mathbf{r}_{\mathbf{m}s}(\tau_e-\tau) \tag{7}$$

which, when synchronized with $\tau = \tau_e$ and $\varphi = \varphi_e$ yield:

$$\mathbf{r_{xc}}(\tau_e,\varphi_e) = \sqrt{\sigma_s^2}\mathbf{a} + \frac{1}{\sqrt{\sigma_s^2}}\boldsymbol{\alpha}_0$$

Thus, when the received and reference signal are synchronized in this way, we can solve for $\boldsymbol{\alpha}_0$:

$$\boldsymbol{\alpha}_0 = (\mathbf{r_{xc}}(\tau_e,\varphi_e) - \sqrt{\sigma_s^2}\mathbf{a})\sqrt{\sigma_s^2}$$

Although we obviously do not know the values of delay and phase that achieve synchronization, we can change the delay τ and phase φ deliberately and compute:

$$\boldsymbol{\alpha}(\tau,\varphi) := (\mathbf{r_{xc}}(\tau,\varphi) - \sqrt{\sigma_s^2}\mathbf{a})\sqrt{\sigma_s^2} \tag{8}$$

which gives us a parametrisation for $\boldsymbol{\alpha}$ that verifies $\boldsymbol{\alpha}(\tau_e,\varphi_e) = \boldsymbol{\alpha}_0$.

Now, we solve the following 2-dimensional minimization problem in order to estimate $\boldsymbol{\alpha}_0$:

$$\min_{\tau,\varphi} \text{rank}(\,\mathbf{C_{xx}} - \mathbf{a}\boldsymbol{\alpha}(\tau,\varphi)^H - \boldsymbol{\alpha}(\tau,\varphi)\mathbf{a}^H\,) \tag{9}$$

The following theorem tells us which are the solutions to (9).

Theorem 1. *In the non-coherent multipath case, the minimum of (9) is attained at the unique point $(\tau,\varphi) = (\tau_e,\varphi_e)$. In the coherent multipath case, the minimum is attained at multiple points, and the ones with the smallest τ correspond to the pairs (τ,φ) with $\tau = \tau_e$ regardless of the value of φ.*

Proof. First assume that $\text{rank}(\mathbf{C_{xx}} - \mathbf{a}\boldsymbol{\alpha}(\tau,\varphi)^H - \boldsymbol{\alpha}(\tau,\varphi)\mathbf{a}^H)$ is minimum. Using Lemma 1, we have that $\boldsymbol{\alpha}(\tau,\varphi)$ satisfies:

$$\begin{aligned}\boldsymbol{\alpha}(\tau,\varphi) &= \boldsymbol{\alpha}_0 - q\mathbf{a} - \mathbf{BR_m p} \\ &= \mathbf{B}\mathbf{r}_{\mathbf{m}s} - q\mathbf{a} - \mathbf{BR_m p} \\ &= -q\mathbf{a} - \mathbf{B}(\mathbf{R_m p} - \mathbf{r}_{\mathbf{m}s})\end{aligned} \tag{10}$$

Substituting (7) in (8), we also have:

$$\begin{aligned}\boldsymbol{\alpha}(\tau,\varphi) &= \left[r_s(\tau_e-\tau)\mathbf{a} + \frac{e^{j(\varphi_e-\varphi)}}{\sqrt{\sigma_s^2}}\mathbf{B}\mathbf{r}_{\mathbf{m}s}(\tau_e-\tau) - \sqrt{\sigma_s^2}\mathbf{a} \right]\sqrt{\sigma_s^2} \\ &= (r_s(\tau_e-\tau)e^{j(\varphi_e-\varphi)} - \sigma_s^2)\mathbf{a} + \mathbf{B}\mathbf{r}_{\mathbf{m}s}(\tau_e-\tau)e^{j(\varphi_e-\varphi)}\end{aligned} \tag{11}$$

Then, comparing (10) and (11), and using that $\mathbf{a}$ and $\mathbf{b}_1, \dots, \mathbf{b}_D$ are linearly independent, results in:

$$\begin{aligned}-q\mathbf{a} &= (r_s(\tau_e-\tau)e^{j(\varphi_e-\varphi)} - \sigma_s^2)\mathbf{a} \\ -\mathbf{B}(\mathbf{R_m p} - \mathbf{r}_{\mathbf{m}s}) &= \mathbf{B}\mathbf{r}_{\mathbf{m}s}(\tau_e-\tau)e^{j(\varphi_e-\varphi)}\end{aligned}$$

which, solving for q, leads to:

$$q = \sigma_s^2 - r_s(\tau_e-\tau)e^{j(\varphi_e-\varphi)} \tag{12}$$

and solving for $\mathbf{p}$ leads to:

$$\mathbf{R_m p} = \mathbf{r}_{\mathbf{m}s} - \mathbf{r}_{\mathbf{m}s}(\tau_e-\tau)e^{j(\varphi_e-\varphi)} \tag{13}$$

With this information at hand, now we can exploit the fact that $\mathbf{p}^H\mathbf{R_m p} = 2\mathcal{R}\{q\}$, as stated by Lemma 1, and we obtain:

$$\begin{aligned}&2\sigma_s^2 - 2r_s(\tau_e-\tau)\cos(\varphi_e-\varphi) \\ &= (\,\mathbf{r}_{\mathbf{m}s}^H - \mathbf{r}_{\mathbf{m}s}^H(\tau_e-\tau)e^{-j(\varphi_e-\varphi)}\,)\,\mathbf{R_m^+}\,(\,\mathbf{r}_{\mathbf{m}s} - \mathbf{r}_{\mathbf{m}s}(\tau_e-\tau)e^{j(\varphi_e-\varphi)})\end{aligned} \tag{14}$$

While we expect $\mathbf{R_m}$ to be generically invertible for the GNSS application, in other applications it may not be full rank, and so to be more general we use the pseudoinverse $\mathbf{R_m^+}$ here.

Eq. (14) shows us a necessary and sufficient condition for the minimization of $\text{rank}(\,\mathbf{C_{xx}} - \mathbf{a}\boldsymbol{\alpha}(\tau,\varphi)^H - \boldsymbol{\alpha}(\tau,\varphi)\mathbf{a}^H\,)$. In practice, this condition must be rewritten using the sample averages $\mathbf{R_m} = (1/N)\mathbf{M^H M}$, $\mathbf{r}_{\mathbf{m}s}(\tau) = (1/N)\mathbf{M^H s}(\tau)$ and $r_s(\tau) = (1/N)\mathbf{s}^H\mathbf{s}(\tau)$ from a set of N consecutive samples, where $\mathbf{M} = [\mathbf{m}[1]\dots\mathbf{m}[N]]^H$ and $\mathbf{s}(\tau) = [s[1+\tau]\dots s[N+\tau]]^H$. With this notation, the condition (14) can be transformed to:

$$\|\mathbf{s} - \mathbf{s}(\tau_e-\tau)e^{j(\varphi_e-\varphi)}\|^2 = \|\mathbf{P_M}(\mathbf{s} - \mathbf{s}(\tau_e-\tau)e^{j(\varphi_e-\varphi)})\|^2 \tag{15}$$

where $\mathbf{P_M} = \mathbf{M}(\mathbf{M^H M})^+\mathbf{M^H}$ is the projection matrix onto the subspace defined by the columns of $\mathbf{M}$. The two possible solutions of (15) are $\mathbf{s} - \mathbf{s}(\tau_e-\tau)e^{j(\varphi_e-\varphi)} = \mathbf{0}$ and $\mathbf{s} - \mathbf{s}(\tau_e-\tau)e^{j(\varphi_e-\varphi)} \in \text{span}\{\mathbf{M}\}$. Note that the first solution is valid for any possible type of multipath, since it does not depend on the matrix $\mathbf{M}$, and it is equivalent to $\mathbf{s} = \mathbf{s}(\tau_e-\tau)e^{j(\varphi_e-\varphi)}$, which gives $\tau = \tau_e$ and $\varphi = \varphi_e$. In contrast, the second solution is only valid if $\mathbf{s} \in \text{span}\{\mathbf{M}\}$, or equivalently, if one or more multipaths have zero relative delay. In this case, we have that $\mathbf{s}(\tau_e-\tau)e^{j(\varphi_e-\varphi)} \in \text{span}\{\mathbf{M}\}$, which gives $\tau = \tau_e + \tau_k$ for $k = 1, \dots, D$ regardless of the value of φ, if we denote the relative delay of the kth multipath by τ_k. Among all these solutions, the ones with the smallest τ correspond to the pairs (τ,φ) with $\tau = \tau_e$. □

From Theorem 1, we know that $\boldsymbol{\alpha}_0$ can be obtained from the unique point (τ_e,φ_e) that minimizes (9) in a scenario with non-coherent multipath. On the other hand, when one or more multipaths are coherent with the direct signal, vectors of the type

$\boldsymbol{\alpha}(\tau_e, \varphi) : \varphi \in [-\pi, \pi]$ are obtained from the points that minimize (9) with the smallest τ. Taking into account these two possible situations, in the following section we discuss the final implementation of the Power-Based Capon beamformer.

4.2. Implementation

As we have introduced at the beginning of Section 4, the idea behind the Power-Based Capon beamformer is to estimate the cross-correlation vector $\boldsymbol{\alpha}_0$ and calculate $\mathbf{R_{xx}} - \mathbf{a}\boldsymbol{\alpha}_0^H - \boldsymbol{\alpha}_0\mathbf{a}^H$. Then, the resulting matrix is treated as the correlation matrix used to calculate the Capon weights. Given that the solution to (2) is:

$$\mathbf{w}_{\text{cap}} = \frac{\mathbf{R_{xx}}^{-1}\mathbf{a}}{\mathbf{a}^H\mathbf{R_{xx}}^{-1}\mathbf{a}} \tag{16}$$

the resulting PBC beamformer is:

$$\mathbf{w}_{\text{pbc}} = \frac{(\mathbf{R_{xx}} - \mathbf{a}\boldsymbol{\alpha}_0^H - \boldsymbol{\alpha}_0\mathbf{a}^H)^{-1}\mathbf{a}}{\mathbf{a}^H(\mathbf{R_{xx}} - \mathbf{a}\boldsymbol{\alpha}_0^H - \boldsymbol{\alpha}_0\mathbf{a}^H)^{-1}\mathbf{a}} \tag{17}$$

In the non-coherent multipath case, we have already seen that $\boldsymbol{\alpha}_0$ is estimated from the unique solution of (9). However, in the coherent multipath case, any vector $\boldsymbol{\alpha}(\tau_e, \varphi)$ is obtained regardless of the value of φ. In order to understand the effect of using an arbitrary value of φ, observe that the resulting correlation matrix $\mathbf{R_{xx}} - \mathbf{a}\boldsymbol{\alpha}(\tau_e, \varphi)^H - \boldsymbol{\alpha}(\tau_e, \varphi)\mathbf{a}^H$ can be written as the sum of $\sigma_s^2\mathbf{a}\mathbf{a}^H$ plus another term corresponding to the correlation matrix of $\mathbf{a}s[n](1 - e^{j(\varphi_e - \varphi)}) + \mathbf{Bm}[n] + \mathbf{v}[n]$. As a result, the PBC beamformer must cancel $s[n](1 - e^{j(\varphi_e - \varphi)})$ with $\mathbf{m}[n]$ in order to minimize the output power, that is:

$$\mathbf{w}_{\text{pbc}}^H\mathbf{a}s[n](1 - e^{j(\varphi_e - \varphi)}) + \mathbf{w}_{\text{pbc}}^H\mathbf{Bm}[n] = 0$$

Then, when we apply w_{pbc} to the actual scenario of Eq. (1), the resulting signal at the output is:

$$y[n] = \mathbf{w}_{\text{pbc}}^H\mathbf{x}[n] = s[n]e^{j(\varphi_e - \varphi)} + \mathbf{w}_{\text{pbc}}^H\mathbf{v}[n]. \tag{18}$$

That is, $s[n]$ is distorted by a factor $e^{j(\varphi_e - \varphi)}$, but the multipaths are eliminated. This behaviour is clearly better than the behaviour of the traditional Capon. Furthermore, if we set $\varphi = 0$, then we guarantee that the resulting distortion is always equal to $e^{j\varphi_e}$, which corresponds to the standard carrier-phase synchronisation error of the GNSS receiver. In this way, we do not perform any additional correction in the estimated carrier-phase, but we assure that the proposed methodology does not worsen the performance of the system. Algorithm 1 summarizes the whole process:

Finally note that, in order to implement the proposed methodology, a cost function that properly approximates the rank needs to be chosen to avoid errors caused by the use of numerical rank. A typical choice found in the literature is the nuclear norm [34], because it is a convex approximation to the rank and it leads to the optimal solution under some optimality conditions. However, simulations show that in this work it is necessary to use a more precise heuristic to approximate the rank. Since there are only two independent variables τ and φ in (9), which take values in very small intervals of $\mathbb{R}$, in practice it makes sense to perform a two-dimensional grid search. This opens the doors to use non-convex approximations such as the so-called Schatten p-norm. This norm can be understood as a generalisation of the nuclear norm, and it is defined as:

$$\|\mathbf{Q}\|_p = \left(\sum_k \sigma_k^p(\mathbf{Q})\right)^{\frac{1}{p}} \quad \text{with} \quad 1 \le p < \infty \tag{19}$$

where $\mathbf{Q} \in \mathbb{C}^{N \times N}$, and $\sigma_k(\mathbf{Q})$ is the kth eigenvalue of $\mathbf{Q}$. Note that the Schatten p-norm corresponds to the nuclear norm for $p = 1$.

The definition (19) also includes the Frobenius norm $\|\mathbf{Q}\|_2$ and the spectral norm $\|\mathbf{Q}\|_\infty$, and with special interest here, it can be extended to $p \in (0, 1)$. If it is extended, then the Schatten p-norm becomes a quasinorm, but we can exploit the fact that $\|\mathbf{Q}\|_p$ to the power of p tends to rank($\mathbf{Q}$) when $p \to 0$. Indeed, raising $\|\mathbf{Q}\|_p$ to the power of p does not change the points where the minimum is attained. Then, the lower the value of p, the closer to the minimum rank solution. In practice, however, very low values of p are not recommended, since they can increase significantly the contribution of those singular values that are not exactly zero but correspond to the null space of $\mathbf{Q}$. As a result, an intermediate value must be chosen instead. In the results presented in the following section, we have used $p = 0.2$.

Algorithm 1 PBC Beamforming.

Given the received signal $\mathbf{x}[n]$ and local reference $c[n]$

1) Calculate $\mathbf{R_{xx}}$ and $\mathbf{r}_{\mathbf{x}c}(\tau, \varphi)$

2) Obtain $\mathbf{C_{xx}}$ and $\boldsymbol{\alpha}(\tau, \varphi)$

3) Solve $\arg\min_{\tau,\varphi} \text{rank}(\, \mathbf{C_{xx}} - \mathbf{a}\boldsymbol{\alpha}(\tau, \varphi)^H - \boldsymbol{\alpha}(\tau, \varphi)\mathbf{a}^H \,)$

if solution is not unique **then**

  take the one with smallest τ and $\varphi = 0$

end if

4) Obtain corresponding $\boldsymbol{\alpha}(\tau, \varphi)$

5) Compute $\mathbf{w}_{\text{pbc}}$ using $\boldsymbol{\alpha}_0 = \boldsymbol{\alpha}(\tau, \varphi)$

5. Simulation results

In this section, we present some numerical examples related to the implementation of the proposed PBC beamformer. In order to show the effectiveness of the methodology, we have first calculated the response of the beamformer to multipath and noise, and we plot the results together with those of other representative methodologies. In addition, we have also calculated the time-delay and carrier-phase of the direct signal that are obtained after applying these beamforming techniques, and the output error is represented. For this purpose, we have used a Delay-Locked Loop (DLL) and a Phase-Locked Loop (PLL), but note that any other specific technique can be used after beamforming, including one that exploits the temporal diversity of the multipath as in [6–8].

Throughout all the simulations, we assume that a linear antenna array receives a Global Positioning System (GPS) signal and several multipath reflections, and that $C/N_0 = 45$ dBHz. The corresponding post-despreading versions of the signals have been calculated from a triangle function of duration $t_c = 1/1023$ ms, with a given delay, amplitude and phase specified in each figure. This triangle function has also been used to generate the filtered additive white Gaussian noise. Then, we assume that $N_\text{p} = 31$ samples are taken at each correlation peak, within an interval approximately $\pm t_c$, and centered at the time-delay obtained from the DLL. The integration time of the GPS receiver was set to $T_\text{int} = 20$ ms, and the observation time to $T = 200$ ms. The result of this configuration is $\mathbf{x}[n]$ in (1), from which the beamformer is calculated.

To begin, we evaluate the response of the proposed PBC beamformer to three received multipaths when an 8-element antenna array is used. Fig. 2 plots the expected value of the total multipath power at the output of the beamformer. This power is normalized with respect to the power of the LOSS with the aim of

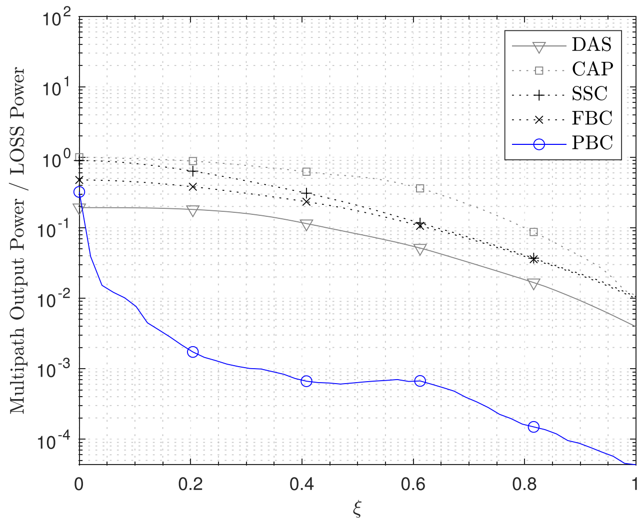

Fig. 2. Multipath response of different beamformers, versus delay factor ξ. The relative powers, delays and phases of the multipaths are given by $\kappa_{\mathbf{m}} = [\,0.9\ \ 0.5\ \ 0.25\,]$, $\tau_{\mathbf{m}} = [\,1.5\ \ 2\ \ 2.5\,]\,t_c$ and $\phi_{\mathbf{m}} = [\,-\pi/4\ \ \pi/2\ \ 0\,]\,$rad respectively. The DOA's of the multipaths and direct signal are -20°, 80°, 0° and 30° respectively.

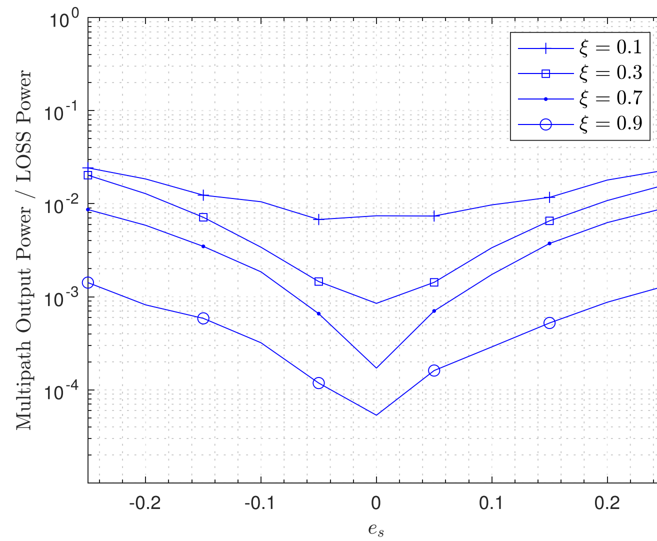

Fig. 3. Multipath response of PBC versus LOSS power estimation error e_s. Each line corresponds to a different value of ξ. The relative powers, delays and phases of the multipaths are given by $\kappa_{\mathbf{m}} = [\,0.9\ \ 0.5\ \ 0.25\,]$, $\tau_{\mathbf{m}} = [\,1.5\ \ 2\ \ 2.5\,]\,t_c$ and $\phi_{\mathbf{m}} = [\,-\pi/4\ \ \pi/2\ \ 0\,]\,$rad respectively. The DOA's of the multipaths and direct signal are -20°, 80°, 0° and 30° respectively.

emphasizingthe LOSS cancellation with the multipaths. In order to get the performance for a broad range of correlations, the delays of the multipaths are defined by the product of a delay factor $\xi \in [0, 1]$ and a vector $\tau_{\mathbf{m}} = [\,1.5\ \ 2\ \ 2.5\,]\,t_c$ containing each maximum multipath delay, and the results are represented as a function of ξ. When ξ is zero, all the multipaths are received coherently, and when $\xi = 1$, they are received with delays given by $\tau_{\mathbf{m}}$. The results corresponding to the Capon (CAP) beamformer are also represented, together with those obtained by additional preprocessing: spatial smoothing (SSC) and forward/backward (FBC). Finally, the Delay-And-Sum (DAS) beamformer is also evaluated, which uses the deterministic weights $\mathbf{w}_{\text{das}} = (1/N)\mathbf{a}$ in all possible scenarios.

As we can see in Fig. 2, the PBC beamformer clearly outperforms the presented methods for all values of ξ. When $\xi = 0$, the exact value of φ_e cannot be estimated from the two-dimensional search given by (9), and $\varphi = 0$ is chosen. Thus, the response to the multipaths is given by the squared absolute value of $1 - e^{j(\varphi_e - 0)}$. In contrast, the response of the CAP beamformer equals one when the delay factor is zero, since the cancellation phenomenon takes place. The DAS beamformer performs then better than CAP at this point. On the other hand, when the delay factor increases, the PBC beamformer immediately mitigates the multipaths, achieving multipath-to-LOSS ratios as low as 10^{-2} for $\xi > 0.1$. The response of the CAP beafmormer is also improved, but not as much as PBC unless the multipaths are completely uncorrelated. For its part, SSC and FBC approaches offer enhanced performance compared to CAP, but they are still far from PBC because they only achieve a small decrease in correlation. Finally, note that the response of the DAS beamformer does not change significantly as a function of ξ, since it is a deterministic beamformer.

In order to provide some insights into the robustness of the proposed technique against possible mismatches between the received power of the LOSS and the corresponding estimated value, the response of the PBC has also been calculated with respect to errors in this estimation. Concretely, Fig. 3 considers the previous scenario and shows the output multipath power as a function of $e_s = (\hat{\sigma}_s^2 - \sigma_s^2)/\sigma_s^2$, where $\hat{\sigma}_s^2$ is used to denote the estimated value of σ_s^2. Different lines correspond to different values of ξ, so that several correlations can be considered. As it could be expected, the greater the mismatch, the more multipath power is present at the output. However, as Fig. 3 shows, the obtained multipath-to-LOSS ratios are about $2 \cdot 10^{-2}$ when the estimation errors are as high as 25% of σ_s^2, and they do not exceed 10^{-2} unless the errors on the estimation are greater than 10%. Then, while precision in power estimation may play an important role in mitigating the multipath effects, the results provided here show that errors as high as 10% may be tolerated with little consequences.

Fig. 4 shows the expected value of the noise power at the output of the beamformer, also normalized with respect to the power of the LOSS. In this case, we notice that the PBC beamformer has a good response for all values of ξ. For its part, the CAP beamformer offers a remarkably higher response than the rest. The reason is that minimization of the output power implies merging the noise with the multipaths, due to the fact that they show some degree of correlation for short sample records. Additional simulations show that this effect can be limited by increasing the time window T, since the noise becomes less correlated. For instance, responses that do not exceed 10^{-2} can be obtained for $T > 1\,$s. This effect is somewhat modified by the SSC and FBC approaches. Finally, the DAS curve shows a lower bound among all beamformers, which is consistent with the fact that it is the beamformer with maximum array gain.

In Fig. 5, we show the expected value of the time-delay estimation error at the DLL when a 5-element antenna array is used. We consider that an early-late tracking loop is configured with an early-minus-late power discriminator [35] and a correlator spacing equal to $t_c/4$. Two multipath reflections with $\tau_{\mathbf{m}} = [\,1.5\ \ 2.5\,]\,t_c$ are received together with the LOSS, and a dashed line is additionally plotted that corresponds to PBC when the reference and received signals are synchronized with $\tau = \tau_e$ and $\varphi = \varphi_e$. As we can see, the most remarkable aspect of the plots is that the PBC curve does not show any significant variation with ξ. In particular, it shows time-delay errors below 3 m for any delay factor. Thus, the case $\xi = 0$ is not critical for the DLL if it is used together with the PBC beamformer. In contrast,

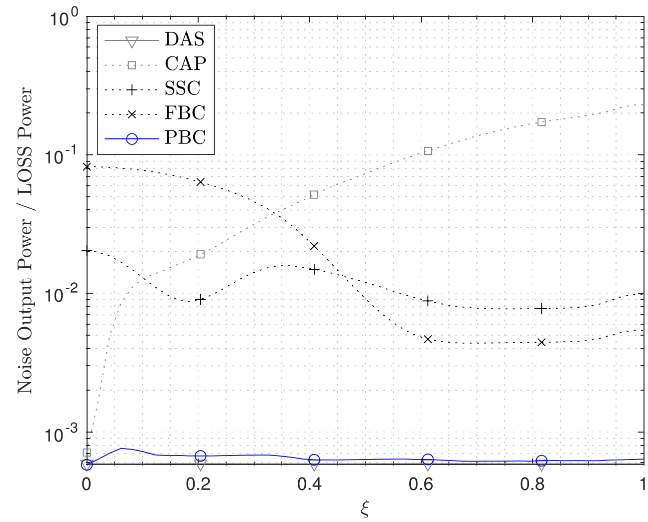

Fig. 4. Noise response of different beamformers, versus delay factor ξ. The relative powers, delays and phases of the multipaths are given by $\kappa_{\mathbf{m}} = [\,0.9\ \ 0.5\ \ 0.25\,]$, $\tau_{\mathbf{m}} = [\,1.5\ \ 2\ \ 2.5\,]\,t_c$ and $\phi_{\mathbf{m}} = [\,-\pi/4\ \ \pi/2\ \ 0\,]$ rad respectively. The DOA's of the multipaths and direct signal are -20°, 80°, 0° and 30° respectively.

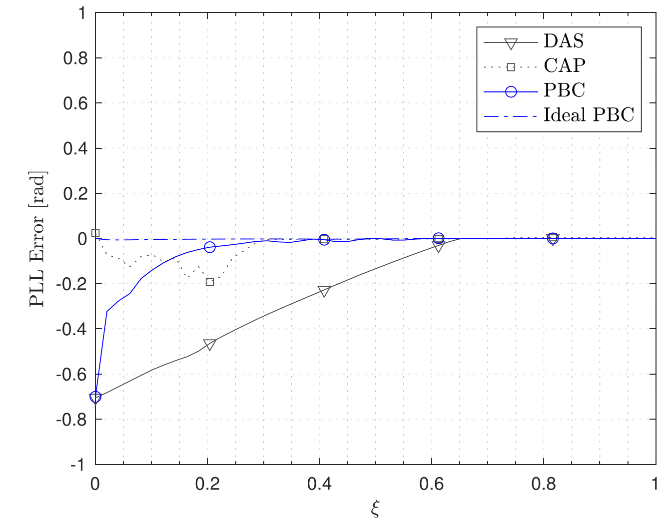

Fig. 6. Output error of a PLL when it is used together with different beamformers, versus delay factor ξ. The relative powers, delays and phases of the multipaths are given by $\kappa_{\mathbf{m}} = [\,0.9\ \ 0.5\,]$, $\tau_{\mathbf{m}} = [\,1.5\ \ 2.5\,]\,t_c$ and $\phi_{\mathbf{m}} = [\,-\pi/4\ \ \pi/2\,]$ rad respectively. The DOA's of the multipaths and direct signal are -20°, 80° and 30° respectively.

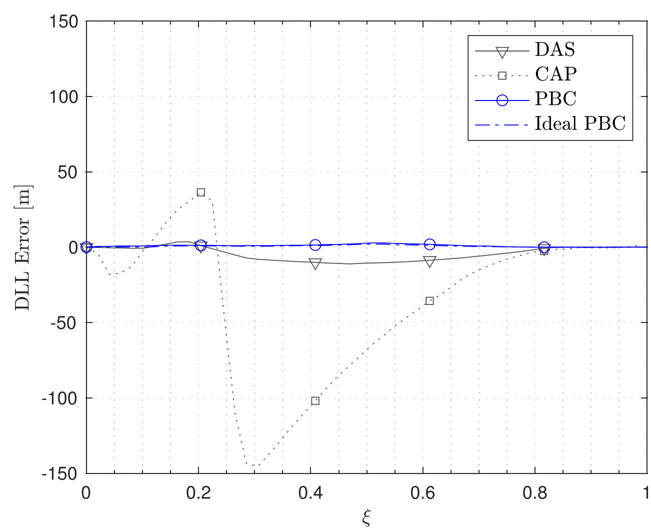

Fig. 5. Output error of a DLL when it is used together with different beamformers, versus delay factor ξ. The relative powers, delays and phases of the multipaths are given by $\kappa_{\mathbf{m}} = [\,0.9\ \ 0.5\,]$, $\tau_{\mathbf{m}} = [\,1.5\ \ 2.5\,]\,t_c$ and $\phi_{\mathbf{m}} = [\,-\pi/4\ \ \pi/2\,]$ rad respectively. The DOA's of the multipaths and direct signal are -20°, 80° and 30° respectively.

the DAS and CAP techniques show large variations with ξ, and they generate errors as high as 145 m. For its part, the shape of the DAS curve is a subtle variation of the curve that would be obtained without beamforming, which happens because this beamformer has a spatial attenuation that does not depend on ξ.

Fig. 6 shows the expected value of the carrier-phase estimation error at the PLL considering that it is calculated from the prompt correlation output and using the previous configuration. In this case, note that the results can be misleading in that the CAP beamformer performs reasonably well, because this technique generates very random phase values for small and medium ξ, and hence they cannot be treated as reliable. This occurs because the multipaths cancel the LOSS, and the noise becomes dominant. For its part, the PBC approach does not perform any additional correction in the carrier-phase when $\xi = 0$, and hence it generates exactly the same phase as the DAS approach. The former, however, performs better when the delay factor increases, allowing for very precise phase estimates when $\xi > 0.1$. In contrast, the DAS beamformer leads to significant errors until the multipaths are received with large relative delays, similarly to what would be obtained without beamforming.

Finally, in order to consider the effect of the multipath phase relative to the LOSS, Figs. 7 and 8 show the delay and phase envelopes of the multipath when a 5-element antenna array is used. They have been calculated as the noiseless time-delay and carrier-phase estimation errors at the DLL and PLL respectively, when just one multipath reflection is received together with the LOSS. The beamformers have been evaluated in two different situations that depict the worst possible cases depending on the value of the relative multipath phase. For a fair comparison, the results corresponding to a single-antenna receiver are also represented, and they are labeled as *traditional*. In Fig. 7, the time-delay error is calculated in the two situations where the multipath is received either constructively or destructively with the LOSS. The plots show that the CAP beamformer may reach time-delay errors that are even worse than the traditional ones, while the time-delay errors of PBC are approximately zero for any multipath delay. For its part, the results of the DAS beamformer are better than the traditional ones, but they show a similar behaviour. In Fig. 8, the carrier-phase error is calculated in the two situations where the multipath is received orthogonally to the total received signal. In this case, both the CAP and PBC beamformers generate very low carrier-phase errors except when $\xi = 0$. At this point, the CAP beamformer generates an error equal to φ_e, since the residual of the cancellation phenomenon becomes significant in the absence of noise. For its part, the DAS beamformer is again better than the traditional case, but it has a similar behaviour.

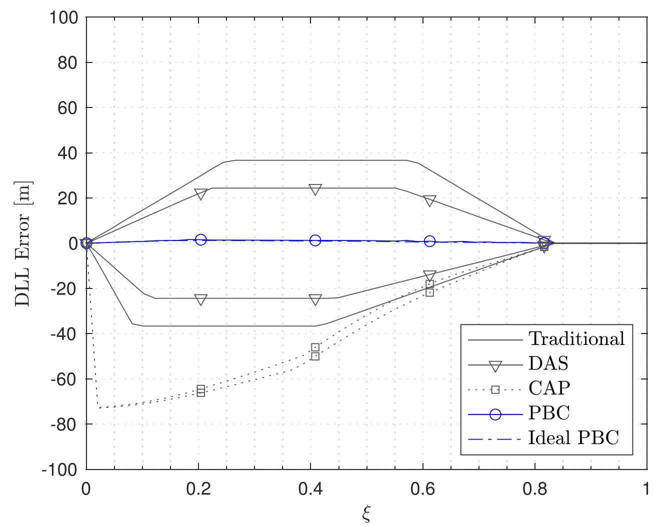

Fig. 7. Multipath delay envelope: worst output error of a DLL when it is used together with different beamformers, versus delay factor ξ. The relative power, delay and phase of the multipath is given by $\kappa_{\mathbf{m}} = 0.25$, $\tau_{\mathbf{m}} = 1.5\,t_c$ and $\phi_{\mathbf{m}} \in \{0, \pi\}$ rad respectively. The DOA's of the multipath and direct signal are -20° and 30° respectively.

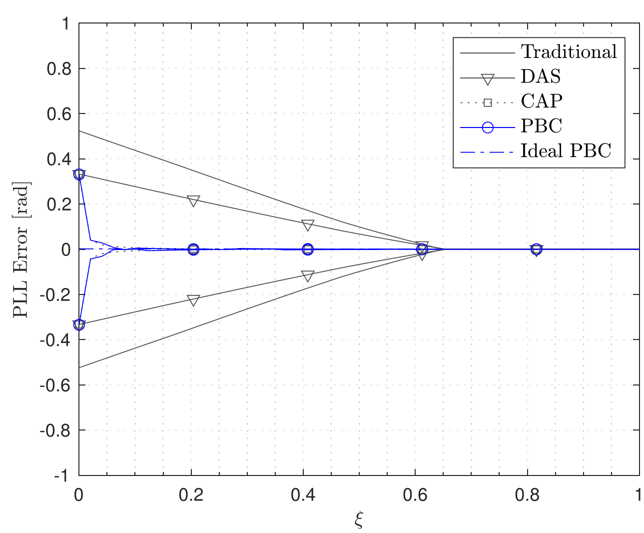

Fig. 8. Multipath phase envelope: worst output error of a PLL when it is used together with different beamformers, versus delay factor ξ. The relative power, delay and phase of the multipath is given by $\kappa_{\mathbf{m}} = 0.25$, $\tau_{\mathbf{m}} = 1.5\,t_c$ and $\phi_{\mathbf{m}} \in \{-2\pi/3, 2\pi/3\}$ rad respectively. The DOA's of the multipath and direct signal are -20° and 30° respectively.

6. Conclusion

In this work, we have proposed a novel data-dependent beamforming technique that is based on the well-known Capon beamformer. This technique aims to avoid the typical cancellation phenomenon between signal and correlated multipaths, and it exploits the fact that the direction-of-arrival and power of the direct signal can be known at the receiver. The proposed procedure first identifies the portion of multipaths that contributes to the cancellation, and then counteracts it before calculating the traditional Capon weights. It involves calculating the spatial correlation matrix of the incoming signal, the cross-correlation between the incoming signal and a reference signal with variable delay and phase, and implementing a two-dimensional minimization problem. The behaviour of this technique was justified mathematically, and was supported by several numerical results. The analysis and simulations indicate two important scenarios depending on the degree of correlation between the signal and multipaths, with the most limiting situation occurring in the coherent multipath case. In either case, the multipath attenuations obtained by PBC are generally superior to those obtained by other existing techniques, and also, the noise response is very satisfactory. Finally, the time-delay and carrier-phase observables obtained after the beamforming stage by a DLL and a PLL are calculated. We show that, while the obtained time-delay error is approximately zero for any multipath delay, the carrier-phase observables strongly depend on the type of scenario. In the coherent multipath case, the proposed technique does not introduce any additional correction in the carrier-phase, and in the non-coherent multipath case, the obtained carrier-phase is significantly better than that obtained by other existing techniques.

Declaration of Competing Interest

The authors declare that they have no known competing financial interests or personal relationships that could have appeared to influence the work reported in this paper.

CRediT authorship contribution statement

Martí Mañosas-Caballú: Conceptualization, Methodology, Software, Formal analysis, Writing - original draft. **A. Lee Swindlehurst:** Conceptualization, Writing - review & editing, Funding acquisition. **Gonzalo Seco-Granados:** Conceptualization, Writing - review & editing, Supervision, Funding acquisition.

References

[1] E.D. Kaplan, C.J. Hegarty, Understanding GPS/GNSS: Principles and Applications, third ed., Artech House, 2017.
[2] B. Hofmann-Wellenhof, H. Lichtenegger, J. Collins, Global Positioning System: Theory and Practice, Springer, 2001.
[3] A.J.V. Dierendonck, P. Fenton, T. Ford, Theory and performance of narrow correlator spacing in a GPS receiver, ION Navig. 39 (3) (1992) 265–283.
[4] L. Garin, F.V. Diggelen, J.-M. Rousseau, Strobe and edge correlator multipath mitigation for code, in: Proc. ION Int. Tech. Meeting of the Sat. Division, Kansas City, MO, 1996, pp. 657–664.
[5] R.D.J.V. Nee, The multipath estimating delay lock loop, in: Proc. IEEE Int. Symp. on Spread Spectrum Tech. and App., Yokohama, Japan, 1992, pp. 39–42.
[6] M.Z.H. Bhuiyan, E.S. Lohan, Advanced multipath mitigation techniques for satellite-based positioning applications, Hindawi Int. Journal of Navig.and Obs. (2010). Article ID 412393
[7] X. Chen, F. Dovis, S. Peng, Y. Morton, Comparative studies of GPS multipath mitigation methods performance, IEEE Trans. Aerosp. Electron. Syst. 49 (3) (2013) 1555–1568.
[8] C. Cheng, J.-Y. Tourneret, An EM-based multipath interference mitigation in GNSS receivers, Signal Process. 162 (2019) 141–152.
[9] H.L.V. Trees, Optimum Array Processing (Part IV of Detection, Estimation, and Modulation Theory), first edition, Wiley-Interscience, 2002.
[10] D.-J. Moelker, E.V.d. Pol, Y. Bar-Ness, Adaptive antenna arrays for interference cancellation in GPS and GLONASS receivers, in: Proc. IEEE PLANS, Atlanta, GA, 1996, pp. 191–198.
[11] M. Manosas-Caballú, J.L. Vicario, G. Seco-Granados, On the performance of deterministic beamformers: a trade-off between array gain and attenuation, Signal Process. 94 (1) (2014) 158–162.
[12] G. Seco-Granados, J.A.F. Rubio, Maximum likelihood propagation-delay estimation in unknown correlated noise using antenna arrays: application to global navigation satellite systems, in: Proc. IEEE ICASSP, Seattle, WA, 1998, pp. 2065–2068.
[13] M. Sgammini, F. Antreich, L. Kurz, M. Meurer, T.G. Noll, Blind adaptive beamformer based on orthogonal projections for GNSS, in: Proc. ION GNSS, Nashville, TN, 2012, pp. 926–935.
[14] R.G. Lorenz, S.P. Boyd, Robust beamforming in GPS arrays, in: Proc. ION Nation. Technic. Meeting, San Diego, CA, 2002, pp. 409–427.
[15] D. Lu, Q. Feng, R. Wu, Survey on interference mitigation via adaptive array processing in GPS, in: Proc. EA PIERS, Cambridge, MA, vol. 2, 2006, pp. 357–362.
[16] H. Zhao, B. Lian, J. Feng, Adaptive beamforming and phase bias compensation for GNSS receiver, J. Syst. Eng. Electron. 26 (1) (2015) 10–18.
[17] C. Fernandez-Prades, J. Arribas, P. Closas, Robust GNSS receivers by array signal processing: theory and implementation, Proc. IEEE 104 (6) (2016) 1207–1220.
[18] S. Daneshmand, G. Lachapelle, Integration of GNSS and INS with a phased array antenna, GPS Solutions 22 (2018). Article num. 3
[19] Y. Hu, S. Bian, B. Li, L. Zhou, A novel array-based spoofing and jamming suppression method for GNSS receiver, IEEE Sens. J. 18 (7) (2018) 2952–2958.

[20] A.L. Swindlehurst, B.D. Jeffs, G. Seco-Granados, J. Li, Applications of array signal processing, in: Academic Press Library in Signal Processing, vol. 3, chapter 20, Elsevier, 2014, pp. 859–953.

[21] B. Widrow, K. Duvall, R. Gooch, W. Newman, Signal cancellation phenomena in adaptive antennas: causes and cures, IEEE Trans. Ant. Prop. 30 (3) (1982) 469–478.

[22] T.-J. Shan, M. Wax, T. Kailath, On spatial smoothing for direction-of-arrival estimation of coherent signals, IEEE Trans. ASSP 33 (4) (1985) 806–811.

[23] Y. Bresler, V.U. Reddy, T. Kailath, Optimum beamforming for coherent signal and interferences, IEEE Trans. ASSP 36 (6) (1988) 833–843.

[24] S.U. Pillai, B.H. Kwon, Forward/backward spatial smoothing techniques for coherent signal identification, IEEE Trans. ASSP 37 (1) (1989) 8–15.

[25] I. Ziskind, M. Wax, Maximum likelihood localization of multiple sources by alternating projection, IEEE Trans. ASSP 36 (10) (1988) 1553–1560.

[26] F. Qian, B.D.V. Veen, Quadratically constrained adaptive beamforming for coherent signals and interference, IEEE Trans. Signal Process. 43 (8) (1995) 1890–1900.

[27] G. Seco-Granados, J.A. Fernandez-Rubio, C. Fernandez-Prades, ML estimator and hybrid beamformer for multipath and interference mitigation in GNSS receivers, IEEE Trans. Signal Process. 53 (3) (2005) 1194–1208.

[28] M.G. Amin, W. Sun, A novel interference suppression scheme for global navigation satellite systems using antenna array, IEEE J. Sel. Areas Commun. 23 (5) (2005) 999–1012.

[29] M. Manosas-Caballú, G. Seco-Granados, A.L. Swindlehurst, Robust beamforming via FIR filtering for GNSS multipath mitigation, in: Proc. IEEE ICASSP, Vancouver, BC, 2013, pp. 4173–4177.

[30] J. Wu, X. Tang, Z. Li, C. Li, F. Wang, Cascaded interference and multipath suppression method using array antenna for GNSS receiver, IEEE Access 7 (2019) 69274–69282.

[31] F.K. Brunner, H. Hartinger, L. Troyer, GPS signal diffraction modelling: the stochastic SIGMA-d model, J. Geodesy 73 (1999) 259–267.

[32] J. Capon, High-resolution frequency-wavenumber spectrum analysis, Proc. IEEE 57 (8) (1969) 1408–1418.

[33] C.D. Meyer, Matrix Analysis and Applied Linear Algebra, first edition, SIAM, 2000.

[34] B. Recht, M. Fazel, P.A. Parrilo, Guaranteed minimum-rank solutions of linear matrix equations via nuclear norm minimization, SIAM Rev. 52 (3) (2010) 471–501.

[35] K. Borre, D.M. Akos, N. Bertelsen, P. Rinder, S.H. Jensen, A Software-Defined GPS and GALILEO Receiver, Birkhaüser, 2007.